

Chemical Science

Accepted Manuscript



This is an *Accepted Manuscript*, which has been through the Royal Society of Chemistry peer review process and has been accepted for publication.

Accepted Manuscripts are published online shortly after acceptance, before technical editing, formatting and proof reading. Using this free service, authors can make their results available to the community, in citable form, before we publish the edited article. We will replace this *Accepted Manuscript* with the edited and formatted *Advance Article* as soon as it is available.

You can find more information about *Accepted Manuscripts* in the [Information for Authors](#).

Please note that technical editing may introduce minor changes to the text and/or graphics, which may alter content. The journal's standard [Terms & Conditions](#) and the [Ethical guidelines](#) still apply. In no event shall the Royal Society of Chemistry be held responsible for any errors or omissions in this *Accepted Manuscript* or any consequences arising from the use of any information it contains.

ARTICLE

DNA-based visual majority logic gate with one-vote veto function

Cite this: DOI: 10.1039/x0xx00000x

Daoqing Fan^{ab}, Kun Wang^{abc}, Jinbo Zhu^{ab}, Yong Xia^{ab}, Yanchao Han^{ab}, Yaqing Liu^{ab*} and Erkang Wang^{ab*}

Received 00th January 2012,
Accepted 00th January 2012

DOI: 10.1039/x0xx00000x

www.rsc.org/chemicalscience

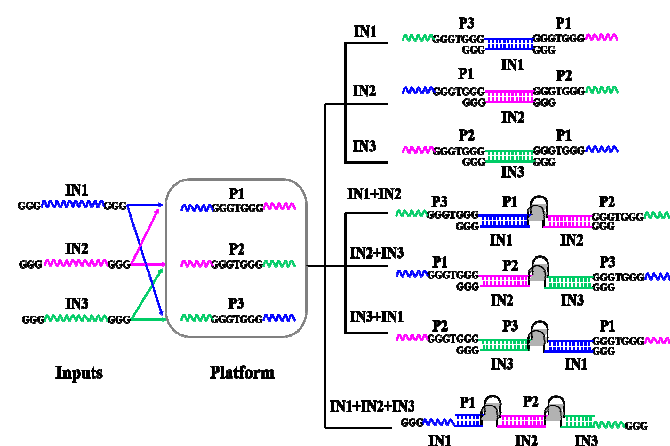
Molecular logic gate is basic element and plays a key role on molecular computing. Herein, we have developed a label-free and enzyme-free three-input visual majority logic gate which is for the first time realized only according to DNA hybridization without DNA replacement and enzyme catalysis. Besides, one-vote veto function was integrated into the DNA-based majority logic gate, in which one input has priority over other inputs. The developed system also can implement multiple basic and cascade logic gates.

Introduction

Untraditional molecular computing is of scientific interesting and has drawn an increasing attention in extensive research fields.¹⁻⁴ Due to the low-cost, feasible synthesis, well-ordered and predictable structure, DNA has been confirmed as excellent building blocks for engineering of biomolecular circuits.⁵⁻⁹ Various basic and advanced DNA-based logic gates have been fabricated by making use of biotechnologies.¹⁰⁻¹⁵ Though great achievements have been obtained, the research on DNA computing is still in an early stage. Herein, our investigation focused on developing a DNA-based majority logic gate. It can be used in fault-tolerant computing and also can serve as versatile building block for constructing reversible logic circuits and advanced logic circuits such as full adder.¹⁶ In 2006, Porod's group reported the first majority logic gate based on magnetic quantum-dot cellular automata technology.¹⁷ Up to now, only three molecular majority logic gate have been experimentally validated according to the delicate design. By taking advantage of biocatalytic reactions operating in parallel an enzyme-based majority gate was realized by Katz's group.¹⁸ Based on toehold-mediated DNA displacement strategy, Liu's group constructed a FAM-labeled majority logic gate.¹⁹ By combining four-way junction (Holiday Junction) and toehold-mediated DNA displacement, an enzyme-free majority logic gate was successfully realized.²⁰

Considering the potential application, a simple operation, low-cost logic gate would present great advantage. Inspired by the previous achievements, herein we developed a label-free three-input majority logic gate just according to DNA hybridization without enzyme or (deoxy)ribozyme catalysis and DNA replacement. In Boolean logic,

a *TRUE* decision can be made by a majority logic gate only when more than half of its inputs present. Otherwise, the majority logic gate makes a *FALSE* decision.²¹ In such a majority logic gate, the three inputs have equal priority. While, some members have priority over the others who can deny the proposal by utilizing the right of one-vote veto, which plays a critical role for final decision. A well-known sample is that the permanent members of the united nation security council have a veto over any proposal. Herein, a visual three-input majority logic gate with one-vote veto function was conceptually developed for the first time. Interestingly, the decision made by the DNA strands not only can be directly distinguished by naked eyes but also can be read with fluorescent signal which may be used as remote output signal.



Scheme 1. The operation principle of the designed three-input majority gate based on DNA hybridization.

Results and discussion

Scheme 1 outlines the operation mechanism of the developed majority logic gate, which is realized just based on hybridization among the input and platform DNA strands. The predictability of Watson-Crick base pairing can simplify the design and implementation of DNA devices.²² Herein, the DNA strands, P1, P2 and P3, function as the platform and the DNA strands, IN1, IN2 and IN3, function as the three inputs. To realize the majority logic function, a split G-quadruplex (2:1:1) strategy is utilized. One G-rich DNA strand is split into three segments, GGGTGGG, GGG and GGG. The segment of GGGTGGG is integrated into the middle of each platform DNA strand (See Platform in Scheme 1). The two GGG segments are integrated into the 3' and 5' terminal of each input, respectively (See Inputs in Scheme 1). The signal transduction is modulated by the formed G-quadruplex (G4) among the platform and input DNA strands. To perform majority logic function, the right part of IN3 can hybridize with the left part of P3, and the left part of IN3 can hybridize with the right part of P2. While, IN3 does not hybridize with P1. The hybridization among the DNA strands was validated by native polyacrylamide gel (PAGE) experiments. As shown in Fig. 1A, the DNA bands of P1, P2, P3 and IN3 appear at a similar position from Lane 1 to Lane 4. After adding IN3 into P2 or P3, new bands appeared in Lane 6 and Lane 7, respectively, indicating the duplex formation of P2/IN3 and P3/IN3. After adding IN3 into P1, no new band appears in lane 5, suggesting no hybridization between IN3 and P1. In the coexistence of P1, P2 and P3, the added IN3 can link P2 and P3 together to produce longer double strand DNA, leading a new band in Lane 8 whose position is quite different from above bands. Another band appears at the position of P1, confirming that the IN3 does not hybridize with P1. Similarly, The IN1 can hybridize with P1 and P3 while not with P2 (See Fig. S1A in SI), the IN2 can hybridize with the platform DNA strands P1 and P2 while does not hybridize with P3 (See Fig. S1B in SI). The sequence of oligonucleotides used in this work was given in Table S1.

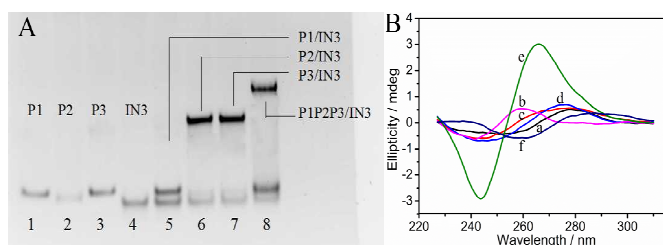


Fig. 1 (A) 15% native polyacrylamide gel analysis of the interaction between IN3 and the platform DNA strands, P1, P2 and P3. Lane 1: P1, Lane 2: P2, Lane 3: P3, Lane 4: IN3, Lane 5: P1+ IN3, Lane 6: P2+IN3, Lane 7: P3+IN3, Lane 8: addition of IN3 into the platform containing P1, P2 and P3. (B) CD spectra of different DNA inputs, platform DNA P1 (a), in the absence of platform with IN1+IN2 (b), in the presence of P1 with IN1 (c), IN2 (d), IN1+IN2 (e) and IN1+IN2+Cu²⁺ (f).

As shown in Scheme 1, no matter which kind of hybridization, no G4 is formed in the presence of each input. When any two inputs are added, G4 is formed. In the addition of IN1 and IN2, the IN1 can hybridize with P1 and P3, and the IN2 can hybridize with P1 and P2. Thus the IN1 and IN2 can be linked together through their hybridization with P1. In other cases, the platform strand P2 can link the IN2 and IN3 together and the P3 can link the IN1 and IN3 together. Thus, all three split parts, GGGTGGG in the platform DNA strands, GGG at terminal of the inputs are integrated together, resulting in the formation of G4. Then it is easily understood that more G4 would be produced in the addition of all three inputs. The design was confirmed by circular dichroism (CD) spectrum measurements with the interaction among P1, IN1, and IN2 as sample. Learned from Fig. 1B, the CD spectra of P1 (curve a) and coexistence of IN1 and IN2 (curve b) are relatively low amplitude, indicating that the DNA strands possess no obvious G4 configuration. After addition of either IN1 (curve c) or IN2 (curve d) into P1, still no obvious G4 configuration was found. While, significant change is monitored once the two inputs, IN1 and IN2, are simultaneously added into P1 (curve e). A positive peak near 265 nm and a negative peak near 243 nm appear, indicating the formation of G4 with a parallel configuration.

Colorimetric logic gates bring convenience for signal readout. According to the above DNA hybridization, a visual majority logic gate was conceptually realized for the first time. Hemin (Fe(III)-protoporphyrin IX) presents high effective peroxidase-like property once binding on G4, forming G4/hemin complex. The complex can catalyze the oxidation reaction between TMB(3,3',5,5'-Tetramethylbenzidine) and H₂O₂.²³⁻²⁷ After stopping the reaction by H₂SO₄, the color of solution is changed from blue to yellow, which can be monitored by naked eyes and is used as output signal. As illustrated in Fig. 2A, in the absence of any input and platform DNA strands, the solution presents pale yellow color, Fig. 2A(a), which is contributed to the oxidation of TMB by H₂O₂. The solution color still keeps pale yellow in the presence of all the platform strands, P1, P2 and P3 (Fig. 2A(b)), indicating that the designed platform strands doesn't catalyze the colorimetric reaction. No obvious color change is monitored after adding any one of the inputs into the platform as shown in Fig. 2A(c-e). In the presence of any two inputs, while, the solution color became bright yellow, Fig. 2A(f-h), thanks to the high catalysis activity of the formed G4/hemin complex on the colorimetric reaction of TMB in the presence of H₂O₂. In the coexistence of all three inputs, more G4/hemin complexes are produced, leading an even dark yellow output, Fig. 2A(i). Herein, the color shown in Fig. 2A(d) is defined as the controlled threshold, the system presents a *TRUE* output (brighter yellow) if more than half inputs exist. Otherwise, the system presents a *FALSE* output (paler yellow). The results fulfill the feature of a majority logic gate, whose decision can be conveniently distinguished by naked eyes. To

establish optimal conditions, the optimized experiments were explored (see Fig. S2 in SI).

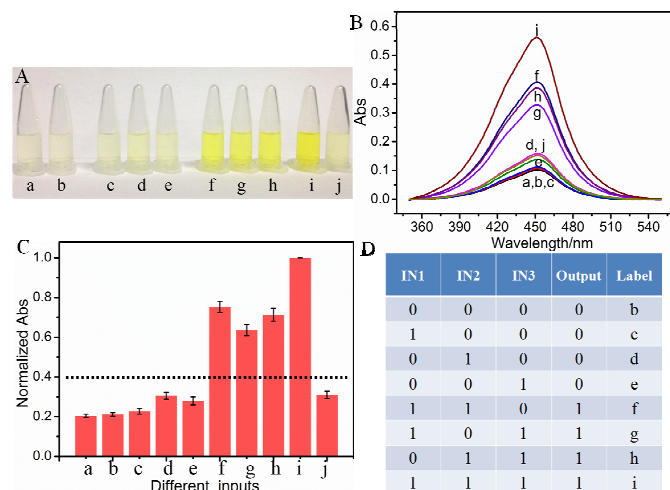


Fig. 2 (A) Photos of the designed majority logic gate with one-vote veto function, (B) UV-vis absorbance curves of (hemin+TMB+H₂O₂) in the absence of any platform and input DNA strands (a), in the presence of platform DNA P1, P2 and P3 (b), in the presence of platform with IN1 (c), IN2 (d), IN3 (e), IN1+IN2 (f), IN2+IN3 (g), IN1+IN3 (h), IN1+IN2+IN3 (i), IN1+IN2+IN3+Cu²⁺ (j) and (C) The normalized absorbance intensity at 450 nm of the designed majority logic gate with one-vote veto function with error bar. Abs of curve i in Fig. 2B was set as 1. Threshold value was set at 0.4 to judge the output signals. The error bar was obtained according to three independent experimental results. (D) The truth table of the three-input majority logic gate.

To further confirm the results, the absorbance values of the system in the presence of various input combinations are detected and shown in Fig. 2B. A low absorbance signal is detected in the absence or presence of only one input, Fig. 2B(a-e). While, an enhanced absorbance signal is detected in the presence of any two or all three inputs, Fig. 2B(f-i), meeting the feature of a three-input majority logic gate. To make it clear, the input “0” and “1” are defined in the absence or presence of respective input. The normalized absorbance response at 450 nm is read as output signal, Fig. 2C. The readout is defined as *TRUE* (1) when the normalized absorbance is higher than a threshold value of 0.40. Otherwise, it is defined as *FALSE* (0). The results generate the truth table as shown in Fig. 2D. It is obvious that the system makes a *TRUE* decision only if more than half of the inputs are introduced, meeting the feature of a majority logic gate. In the absence of the platform, no significant absorbance enhancement is found (See Fig. S3 in SI), indicating that the majority logic function is realized according to the interaction among the inputs and platform. The implementation of the logic function is only based on the interaction among the designed input and platform DNA strands and does not require strand displacement hybridization or enzymatic catalysis, which can reduce the time for signal transmission.^{8, 12}

In a majority logic gate, the inputs have the same priority among each other. While one-vote veto plays an important role in various vote programs, which has never been realized on molecular level. For the first time, herein, we extended a one-vote veto function to the developed majority logic gate. It has been reported that cupric ion can unfold G4 structure as shown in Fig. 1B(f).²⁸ Once Cu²⁺ is added, the G4/hemin complex is correspondingly deformed, significantly reducing the catalysis activity of hemin on the colorimetric reaction. Here Cu²⁺ is introduced as a input, which has priority over the other inputs and can deny the decision made by them. As shown in Fig. 2A(j), the system presents a pale yellow color, which is greatly lighter than that in the presence of all three DNA inputs, validating its priority over the other inputs for the final decision. A low absorbance response further verified what the naked eyes monitored, Fig. 2B(j). The operation of the three-input majority logic gate with one-vote veto function presents high repeatability, which can be found from Fig. 2C.

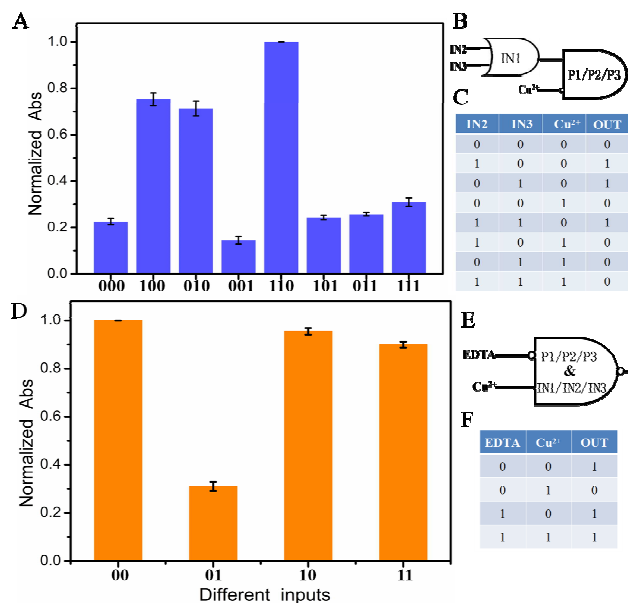


Fig. 3 (A) Normalized Abs at 450 nm of the different input modes of the OR-INHIBIT cascade logic circuit with error bar. Abs at 450 nm of curve i in Fig. 2B was set as 1. Threshold value was set at 0.4 to judge output signals. The input status of IN2, IN3 and Cu²⁺ were represented by three binary numbers, respectively. (B) Diagram of the OR-INHIBIT cascade logic circuit. (C) Truth table of the OR-INHIBIT cascade logic circuit. (D) Normalized Abs at 450 nm of the different input modes of the IMPLICATION logic circuit with error bar. Abs at 450 nm of curve i in Fig. 2B was set as 1. Threshold value was set at 0.4 to judge the output signals. The input status of EDTA and Cu²⁺ were represented by two binary numbers, respectively. (E) Diagram of the IMPLICATION logic circuit. (F) Truth table of the IMPLICATION logic circuit. The error bar was obtained according to three independent experimental results.

To fulfill the requirements of increased computational complexity, a molecular platform capable of performing multiple logic operations is in high demand.^{10, 29, 30} As discussed by Li and coworkers, a three-input majority logic

gate can function as a two-input OR gate if any one of the three inputs exists in the initial platform. It also can function as a two-input AND gate if any one of the three inputs is absent in the initial platform.¹⁹ Except those, the developed system here also can perform cascade logic function. If one of the inputs, for example IN1, is defined as the initial platform and the coexistence of more than two input DNA strands as output “1”, the system would function as an OR logic gate. That is, the output of the OR logic gate presents “1” in the coexistence of IN1 and IN2 or IN1 and IN3 or IN1, IN2 and IN3. In a cascade logic gate, the output of the previous logic gate acts as the input of the next gate. If Cu^{2+} acts as another input, the system presents high output “1” (define the normalized Abs intensity of 0.4 as the threshold value) only when the output of the OR logic gate is “1”. Otherwise it is “0”, which is the feature of an INHIBIT logic gate. An OR-INHIBIT cascade logic gate is then realized, Fig. 3A, B and C. Additionally, by taking advantage of the strong coordination between EDTA (Ethylenediaminetetraacetic acid) and Cu^{2+} , the added EDTA results in the reforming of the G4/hemin complex and recovering the absorbance signal, Fig. S4 (k). An IMPLICATION logic gate is then realized with Cu^{2+} and EDTA as inputs if all the input and platform DNA strands work as the initial state, Fig. 3D, E and F. The system presents low output “0” when only Cu^{2+} presented (define the normalized Abs intensity of 0.4 as the threshold value). Otherwise it is “1”.

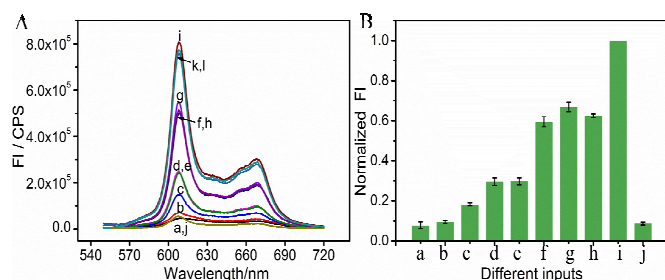


Fig. 4 (A) Fluorescence emission spectra of NMM in the absence of any platform and input DNA strands(a), in the presence of platform DNA P1, P2 and P3(b), in the presence of platform with IN1(c), IN2(d), IN3 (e), IN1+IN2 (f), IN2+IN3 (g), IN1+IN3 (h), IN1+IN2+IN3 (i), IN1+IN2+IN3+ Cu^{2+} (j), P+IN1+IN2+IN3+EDTA (k) and P+IN1+IN2+IN3+ Cu^{2+} +EDTA (l), and (B) The normalized fluorescence intensity at 608 nm of the designed majority logic gate with one-vote veto function with error bar. Fluorescence intensity of curve i in Fig. 4A was set as 1. The error bar was obtained according to three independent experimental results.

Fluorescence signal as output is considered as a multitude of practical applications since the signal enables easy remote reading with low cost.³¹⁻³³ It is worthy to mention that the colorimetric majority logic gate also can be realized with fluorescence as output signal, further confirming the operation repeatability. Here, NMM (N-methylmesoporphyrin IX) was selected as signal reporter, which can bind on G-quadruplex

and produce a significantly enhanced fluorescent signal. Learned from Fig. 4A, a low fluorescence signal was detected in the absence of any input or in the presence of only one of the inputs since no G-quadruplex was formed in the cases. Once any two inputs were added, complex of G-quadruplex/NMM was then formed, generating a significantly enhanced fluorescence of NMM. In the coexistence of all three inputs and the platform, the system presented the highest fluorescent signal. The normalized fluorescence at 608 nm was read as output signal, producing the column bar as a function of various input combinations (Fig. 4B). The output was defined as “1” if the normalized fluorescence is higher than 0.40. Otherwise, it was defined as “0”. It produces the same truth table as given in Fig. 2D, indicating the successful implementation of majority logic gate with the fluorescence signal as output. Once Cu^{2+} was added, the low fluorescent response validates its priority over the other inputs for the final decision, Fig. 4A(j). That is, the system would produce a *FALSE* output once Cu^{2+} was added, confirming the one-vote veto function. The developed system with two kinds of optical signal as output would extend its potential application field.

Conclusions

In conclusion, a DNA-based majority logic gate with one-vote veto function has been successfully realized in a proof-of-principle. The developed logic gate presents several advantages. First, one-vote veto function is integrated into majority logic gate on molecular level for the first time. In the system, one input has priority and can deny the decision made by the other inputs. Second, the logic implementation simply bases on DNA hybridization, reducing the reaction time and simplifying the design. The readout can be conveniently viewed by naked eyes for the first time, which also can be monitored with sensitive fluorescence as output signal. Third, the developed logic gate is label-free and enzyme-free and realized with short oligonucleotide, reducing the cost. Last but not the least, the developed system also can perform multiple basic and cascade logic gates. While, we should be aware that there is still a long road ahead of practical application. The investigation provides a conceptual prototype for constructing multicomponent devices on a single molecular platform.

Experimental Section

Materials

The sequence of oligonucleotides used in this work was given in Table S1. The oligonucleotide was dissolved in water as stock

solution and quantified by UV-vis absorption spectroscopy with the following extinction coefficients ($\epsilon_{260\text{ nm}}$, $\text{M}^{-1}\text{cm}^{-1}$): $A = 15400$, $G = 11500$, $C = 7400$, $T = 8700$. The stock solution of NMM (50 μM) was prepared in dimethyl sulfoxide (DMSO) and stored in darkness at -20°C . The water used in the experiments was purified through a Millipore system. Other chemicals were reagent grade and were used without further purification

Native polyacrylamide gel electrophoresis (PAGE)

10 μM DNA stock solution was diluted to the concentration of 5 μM by an equal volume of 2 \times HEPES buffer (50 mM HEPES, 40 mM KCl, 400 mM NaCl, pH 7.4). HEPES(4-(2-hydroxyethyl)piperazine-1-erhaesulfonic acid) The solution was then heated at 90°C for 10 min and slowly cooled down to room temperature. After that, desired volume of platform and input DNA solution was mixed and suitable volume of 1 \times HEPES buffer (25 mM HEPES, 20 mM KCl, 200 mM NaCl, pH 7.4) was added into the mixture to the final volume of 50 μL . After 30 min's incubation, the DNA solution was analyzed in 15% native polyacrylamide gel. The electrophoresis was conducted in 1 \times TBE (17.80mM Tris, 17.80mM Boric Acid, 2mM EDTA, pH 8.0) at constant voltage of 120 V for 1.5 h. The gels were scanned by a UV transilluminator after staining with Gel-dye.

Circular Dichroism Measurements

CD spectra were measured on a JASCO J-820 spectropolarimeter (Tokyo, Japan) under room temperature. Spectra were recorded from 220 to 320 nm in 1 mm pathlength cuvettes and averaged from three scans.

Operation of the developed majority logic gate

10 μM DNA stock solution was diluted to the concentration of 5 μM by an equal volume of 2 \times HEPES buffer (50 mM HEPES, 40 mM KCl, 400 mM NaCl, pH 7.4), then the solution was heated at 90°C for 10 min and slowly cooled down to room temperature. After that, desired volume of platform and input DNA solution was mixed and suitable volume of 1 \times HEPES buffer (25 mM HEPES, 20 mM KCl, 200 mM NaCl, pH 7.4) was added into the mixture to the final volume of 100 μL . For the cupric ion reaction, desired volume of CuSO_4 was added into the mixed DNA solution. Then an equal volume of 2 \times HEPES buffer (50 mM HEPES, 40 mM KCl, 400 mM NaCl, 0.1% (w/v) Triton X-100, 2% (v/v) DMSO, pH 7.4) was added and incubated for 40 min. Finally, an equal volume of the same concentration of hemin dissolved in the HEPES buffer (25 mM HEPES, 20 mM KCl, 200 mM NaCl, 0.05% (w/v) Triton X-100, 1% (v/v) DMSO, pH 7.4) was added to the solution. The mixture was incubated at room temperature for 1h. The final volume of the sample is 500 μL with a final concentration of 300 nM each platform DNA, 350 nM IN1, 300 nM IN2, 300 nM IN3, 1 μM NMM, 10 μM Cu^{2+} .

Colorimetric reaction

In the oxidation reaction, 10 μL of the final DNAzyme was mixed

with 5 μL 0.5% (w/v) TMB, 5 μL 30% (w/v) H_2O_2 , 480 μL MES-Ac substrate buffer (25 mM MES-Ac, 20 mM KAc, pH 4.5). MES(2-(4-Morpholino)ethanesulfonic acid) An equal volume of 2 M H_2SO_4 was added into the solution after 4 min to stop the reaction. UV-vis absorbance analysis was performed on a Cary 50 Scan UV/Vis/NIR Spectrophotometer (Varian, USA).

Fluorescence spectra measurement

The fluorescence emission spectra of different samples were collected on Fluoromax-4 Spectrofluorometer (HORIBA Jobin Yvon, Inc., NJ, USA) under room temperature from 550 to 750 nm with the excitation wavelength of 399 nm. Slit widths for both the excitation and emission were 3 nm and 5 nm, respectively.

Acknowledgements

This work was supported by the National Natural Science Foundation of China (Nos. 21105095 and 211900040) and State Key Instrument Developing Special Project of Ministry of Science and Technology of China (2012YQ170003), the Instrument Developing Project of the Chinese Academy of Sciences (YZ201203) and the Natural Science Foundation of Jilin Province, China (No. 20130101117JC).

Notes and references

^a State Key Laboratory of Electroanalytical Chemistry, Changchun Institute of Applied Chemistry, Chinese Academy of Sciences, Changchun, Jilin, 130022, PR China

E-mail: yaqingliu@ciac.ac.cn, ekwang@ciac.ac.cn

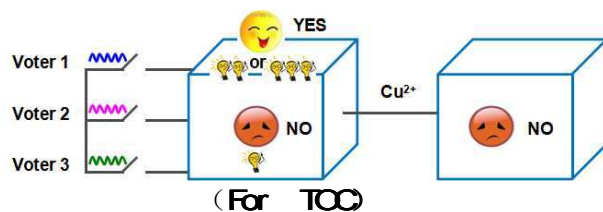
^b University of Chinese Academy of Sciences, Beijing, 100039, China

^c Department of Chemistry and Environmental Engineering, Changchun University of Science and Technology, Changchun, China.

† Electronic Supplementary Information (ESI) available: Table S1 and Fig. S1-S4. See DOI: 10.1039/b000000x/

1. P. A. de Silva, N. H. Q. Gunaratne and C. P. McCoy, *Nature*, 1993, **364**, 42-44.
2. L. Adleman, *Science*, 1994, **266**, 1021-1024.
3. Z. Xie, L. Wroblewska, L. Prochazka, R. Weiss and Y. Benenson, *Science*, 2011, **333**, 1307-1311.
4. D. C. Magri, G. J. Brown, G. D. McClean and A. P. de Silva, *J. Am. Chem. Soc.*, 2006, **128**, 4950-4951.
5. A. J. Genot, J. Bath and A. J. Turberfield, *J. Am. Chem. Soc.*, 2011, **133**, 20080-20083.
6. D. Han, Z. Zhu, C. Wu, L. Peng, L. Zhou, B. Gulbakan, G. Zhu, K. R. Williams and W. Tan, *J. Am. Chem. Soc.*, 2012, **134**, 20797-20804.
7. H. Li, W. Hong, S. Dong, Y. Liu and E. Wang, *ACS Nano*, 2014, **8**, 2796-2803.
8. B. Shlyahovsky, Y. Li, O. Lioubashevski, J. Elbaz and I. Willner, *ACS Nano*, 2009, **3**, 1831-1843.
9. W. Hong, Y. Du, T. Wang, J. Liu, Y. Liu, J. Wang and E. Wang, *Chem. Eur. J.*, 2012, **18**, 14939-14942.
10. S. Xu, H. Li, Y. Miao, Y. Liu and E. Wang, *NPG Asia Mater.*, 2013, **5**, e76.
11. R. Orbach, F. Remacle, R. D. Levine and I. Willner, *Chem. Sci.*, 2014, **5**, 1074-1081.
12. A. Lake, S. Shang and D. M. Kolpashchikov, *Angew. Chem., Int. Ed.*, 2010, **49**, 4459-4462.

13. S. Bi, Y. Yan, S. Hao and S. Zhang, *Angew. Chem., Int. Ed.*, 2010, **49**, 4438-4442.
14. T. Li, D. Ackermann, A. M. Hall and M. Famulok, *J. Am. Chem. Soc.*, 2012, **134**, 3508-3516.
15. R. Orbach, S. Lilienthal, M. Klein, R. D. Levine, F. Remacle and I. Willner, *Chem. Sci.*, 2014, In Press, DOI: 10.1039/C4SC02930E.
16. X. Yang, L. Cai and Q. Kang, *J. Comput. Theor. Nanos.*, 2012, **9**, 621-625.
17. A. Imre, G. Csaba, L. Ji, A. Orlov, G. H. Bernstein and W. Porod, *Science*, 2006, **311**, 205-208.
18. S. Mailloux, N. Guz, A. Zakharchenko, S. Minko and E. Katz, *J. Phys. Chem. B*, 2014, **118**, 6775-6784.
19. W. Li, Y. Yang, H. Yan and Y. Liu, *Nano lett.*, 2013, **13**, 2980-2988.
20. J. Zhu, L. Zhang, S. Dong and E. Wang, *ACS Nano*, 2013, **7**, 10211-10217.
21. M. Goldmann and M. Karpinski, *SIAM J. Comput.*, 1998, **27**, 230-246.
22. G. Seelig, D. Soloveichik, D. Y. Zhang and E. Winfree, *Science*, 2006, **314**, 1585-1588.
23. Y. Xiao, V. Pavlov, T. Niazov, A. Dishon, M. Kotler and I. Willner, *J. Am. Chem. Soc.*, 2004, **126**, 7430-7431.
24. Y. Li and D. Sen, *Nat. Struct. Mol. Biol.*, 1996, **3**, 743-747.
25. T. Li, L. Shi, E. Wang and S. Dong, *Chem. Eur. J.*, 2009, **15**, 3347-3350.
26. J. Zhu, T. Li, L. Zhang, S. Dong and E. Wang, *Biomaterials*, 2011, **32**, 7318-7324.
27. E. Golub, R. Freeman and I. Willner, *Angew. Chem., Int. Ed.*, 2011, **50**, 11710-11714.
28. D. Monchaud, P. Yang, L. Lacroix, M. P. Teulade-Fichou and J. L. Mergny, *Angew. Chem., Int. Ed.*, 2008, **47**, 4858-4861.
29. A. Okamoto, K. Tanaka and I. Saito, *J. Am. Chem. Soc.*, 2004, **126**, 9458-9463.
30. R. Orbach, F. Wang, O. Lioubashevski, R. D. Levine, F. Remacle and I. Willner, *Chem. Sci.*, 2014, **5**, 3381-3387.
31. W. A. L. van Otterlo, E. L. Ngidi and C. B. de Koning, *Tetrahedron Lett.*, 2003, **44**, 6483-6486.
32. Q.-C. Wang, D.-H. Qu, J. Ren, K. Chen and H. Tian, *Angew. Chem., Int. Ed.*, 2004, **43**, 2661-2665.
33. D. H. Qu, Q. C. Wang, X. Ma and H. Tian, *Chem. Eur. J.*, 2005, **11**, 5929-5937.



A label-free and enzyme-free three-input majority logic gate with one-vote veto function